KINETICS OF PARTLY DIFFUSION-CONTROLLED REACTIONS XV: NON-UNIFORM QUENCHER DISTRIBUTION FUNCTION RESULTING FROM DOUBLE ENERGY TRANSFER

J. RIMA†, J. C. ANDRE, F. BAROS and M. BOUCHY

Groupe de Recherches et Applications en Photophysique et Photochimie de l'Unité Associée 328 du Centre National de la Recherche Scientifique, 1 rue Grandville, Ecole Nationale Supérieure des Industries Chimiques, Institut National Polytechnique de Lorraine, 54042 Nancy Cedex (France)

(Received July 20, 1985)

Summary

In some systems, the donor in a triplet–triplet energy transfer can be sensitized in its singlet state through a singlet–singlet energy transfer (Dexter mechanism), where the donor is the acceptor in the triplet transfer itself. As a consequence, an extra acceptor molecule in the triplet energy transfer is present in the vicinity of the donor, thus enhancing the efficiency of the transfer process. Experiments clearly show this effect and a diffusional model using concepts from the physics of simple liquids gives good agreement with the experimental data.

1. Introduction

It is well known that the overall rate of destruction for many initiators decreases with increasing viscosity of the medium [1]. This effect has been interpreted in terms of radical pair formation and several models have been developed. In a recent paper [2], we presented a simple kinetic model representing the recombination of two reactive species in a solvent cage in which we were led to suppose that, at the moment when the two interacting species are formed, there exists an excess of energy which causes their separation at a mean distance greater than the reaction distance.

A similar process occurs in reactions involving electronic energy transfer, in which the kinetics is nearly diffusion controlled [3], and in which two successive transfer reactions occur (Fig. 1). Indeed, when $B^*(S_1)$ is created in the reaction

$$A^*(S_1) + B \longrightarrow A + B^*(S_1)$$

†Permanent address: Université libanaise, Faculté des Sciences II, Mansourieh el Metn, Lebanon.

0047-2670/86/$3.50

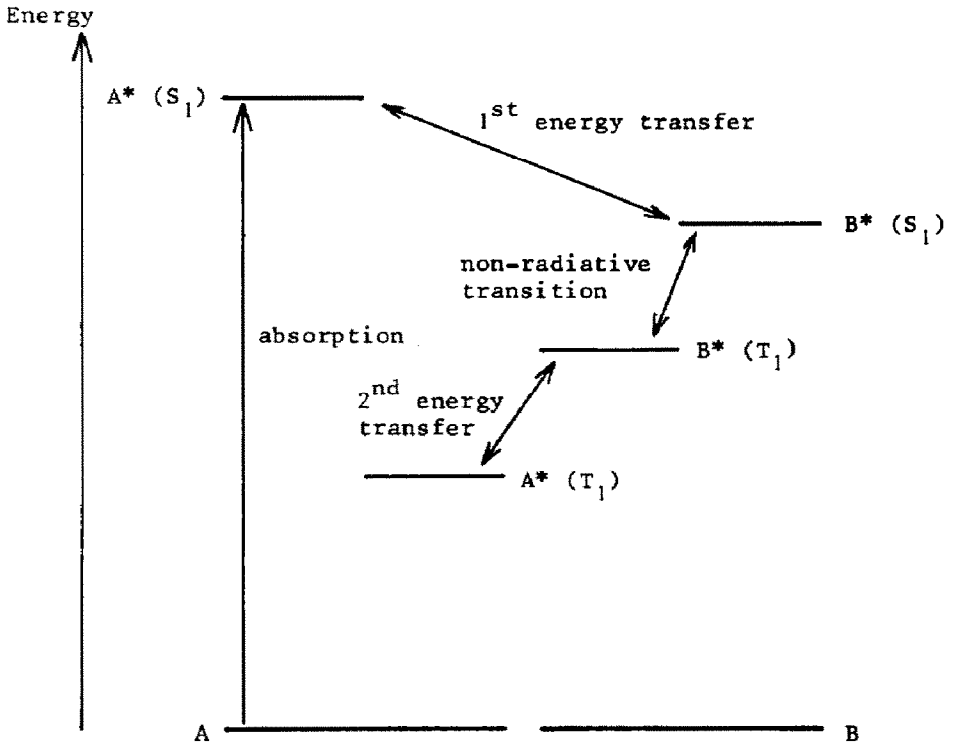

Fig. 1. Scheme for the double energy transfer reaction.

with a sufficiently fast intersystem transition reaction $B^*(S_1) \rightarrow B^*(T_1)$, the configurational distribution of A around $B^*(T_1)$ can no longer be assumed constant. Indeed, if this were so, the A molecule, which had carried the electronic energy before the transfer, would not have enough time to diffuse into the available space and remains in the neighbourhood of $B^*(T_1)$.

Under these conditions, the kinetics of the reaction

$$B^*(T_1) + A \longrightarrow B + A^*(T_1)$$

between $B^*(T_1)$ and A must be enhanced compared with a situation in which the configurational distribution of A is uniform.

Initially we developed a simple model, which is briefly summarized below, and we checked it using pyrene as A and biacetyl as B [4]. These preliminary experiments and models enabled us to show that the configurational distribution of B is altered and that it is consistent with the distribution found in a cage reaction. We have tried to improve the theoretical model by including concepts from liquid physics. However, in view of the mathematical complexity of the problem, we have proposed a simplification of the reaction system; this has allowed us to obtain a relationship which can be used by the experimentalist. Moreover, in order to verify the experimental validity of the model, we have considered other emitting chromophores whose singlet and triplet states are of energies above and below those of biacetyl: 1,2-benzanthracene, 9,10-diphenylanthracene and 1,2,5,6-dibenzanthracene. These different experiments point out the general validity of the simplification and

can be interpreted with success using the models developed. In this paper we first give a mathematical description of the system and then describe the use of the models to fit the experimental results.

2. Modelling of the transfer kinetics

2.1. Simple model

Let us first consider a mean concentration of A sufficiently small that the quenching reaction can be assumed to be the sum of two reactions: (a) a reaction originating mainly from a set of A molecules in the enlarged cage around $B(T_1)$; (b) a reaction originating from a quencher molecule placed outside the cage.

The experimental results below show that it is possible for such a situation to exist. The deactivation of $B(T_1)$ by the classical process based on a constant configurational distribution of A is very similar. We have determined the yield of deactivation of $B(T_1)$ by A molecules by the electronic energy transfer reaction

$$A(S_1) + B \longrightarrow B(S_1) + A$$

Consider an A molecule, created at time $t = 0$, close to $B^*(S_1)$ at the reaction distance σ. If the two molecules do not react, A will diffuse into the medium following the classical law

$$\frac{\partial \varphi}{\partial t} = D \nabla^2 \varphi$$

(with no potential) [2] where D is the mutual diffusion coefficient of A and B and φ is the local concentration of B.

If y is the Laplace transform of φ

$$y(s) = \int_0^\infty \exp(-s\tau)\varphi(\tau)\, d\tau$$

with $\tau = Dt/\sigma^2$, normalization gives

$$y(s) = \frac{1}{NV_0} \frac{1}{1 + s^{1/2}} \frac{\exp\{-s^{1/2}(\rho - 1)\}}{\rho}$$

where ρ is the ratio (distance of A from $B^*(S_1)$)/σ, N is Avogadro's number and $V_0 = 4\pi\sigma^3$.

Defining a rate constant k_0 for the monomolecular relaxation of $B^*(S_1)$ to $B^*(T_1)$, it is possible to determine the expression for the mean configurational distribution of A around $B^*(T_1)$ at the time when it is created:

$$\langle \varphi \rangle = \int_0^\infty k_0 \exp(-k_0 t)\varphi(\rho, t)\, d\tau$$

$$= \frac{k_0\sigma^2}{D} \mathcal{L}\{\varphi(\rho,\tau)\}_{k_0\sigma^2/D}$$

If we assume that $B^*(T_1)$ is created at $t = 0$, the configurational distribution of A around it is equal to the value of yK_0 for $s = K_0 = k_0\sigma^2/D$

$$\langle\varphi\rangle = \frac{K_0}{NV_0} \frac{\exp\{-K_0^{1/2}(\rho - 1)\}}{(1 + K_0^{1/2})\rho}$$

If we consider that the function at time τ is $\varphi(\tau)$, we have to solve

$$\frac{\partial\varphi(\tau,\tau')}{\partial\tau'} = \frac{\partial^2\varphi(\tau,\tau')}{\partial\rho^2} + \frac{2}{\rho}\frac{\partial\varphi(\tau,\tau')}{\partial\rho}$$

with given limiting conditions. If $p(\tau)\,d\tau$ is the probability for that particular distribution to occur we can write

$$p(\tau)\,d\tau\frac{\partial\varphi(\tau,\tau')}{\partial\tau'} = p(\tau)\,d\tau\left\{\frac{\partial^2\varphi(\tau,\tau')}{\partial\rho^2} + \frac{2}{\rho}\frac{\partial\varphi(\tau,\tau')}{\partial\rho}\right\}$$

and

$$\int_0^\infty p(\tau)\,d\tau\frac{\partial\varphi(\tau,\tau')}{\partial\tau'} = \int_0^\infty p(\tau)\frac{\partial^2\varphi(\tau,\tau')}{\partial\rho^2}\,d\tau + \frac{2}{\rho}\int_0^\infty p(\tau)\frac{\partial\varphi(\tau,\tau')}{\partial\rho}\,d\tau$$

with $p(\tau) = K_0\exp(-K_0\tau)$. This then becomes

$$\frac{\partial}{\partial\tau'}\mathcal{L}\{\varphi(\tau,\tau')\}_{K_0} = \frac{\partial}{\partial\rho^2}\mathcal{L}\{\varphi(\tau,\tau')\}_{K_0} + \frac{2}{\rho}\frac{\partial}{\partial\rho}\mathcal{L}\{\varphi(\tau,\tau')\}_{K_0}$$

where $\mathcal{L}\{\varphi(\tau,\tau')\}_{K_0}$ is the Laplace transform of $\varphi(\tau,\tau')$ for $s = K_0$. This leads to an initial distribution ($\tau' = 0$) given by

$$\langle\varphi\rangle = \mathcal{L}\{\varphi(\tau,0)\}_{K_0} = \frac{K_0}{NV_0}\frac{\exp\{-K_0^{1/2}(\rho - 1)\}}{(1 + K_0^{1/2})\rho}$$

and to a corresponding time evolution. Figure 2 shows, as an example, the variations in the configuration of A around $B^*(T_1)$ for different values of K_0.

2.1.1. Static quenching

When a chemical reaction between species can occur at a distance larger than the collision distance [3, 5] and when the rate constant $k(r)$ reaches high values, we assume that the rate constant is nearly infinite between σ and a kinetic distance $\sigma' = R\sigma$ ($R > 1$) [3, 6]. Although this model is open to some criticism [7], we have shown that the kinetics of the system was only slightly altered by using such a simple assumption. It also allows the experimental parameters to be easily determined [8]. The yield of the reaction between A and $B(T_1)$, between 1 and R, is expressed by

$$SQ = \frac{K_0\exp(K_0^{1/2})}{1 + K_0^{1/2}}\int_1^R \rho\exp\{-(K_0\rho)^{1/2}\}$$

$$= 1 - \frac{K_0^{1/2}R + 1}{K_0^{1/2} + 1}\exp\{-K_0^{1/2}(R - 1)\}$$

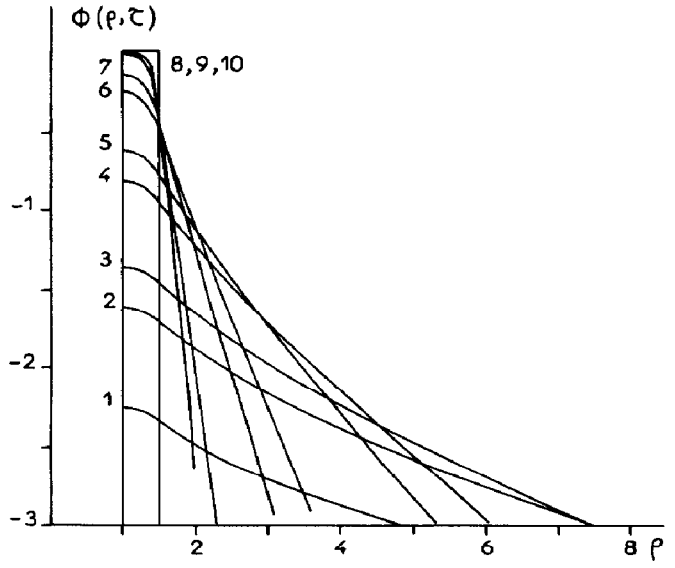

Fig. 2. Variations in the initial configurational distribution function of A around B*(T_1): curve 1, $K_0 = 0.01$; curve 2, $K_0 = 0.05$, curve 3, $K_0 = 0.1$; curve 4, $K_0 = 0.5$; curve 5, $K_0 = 1$; curve 6, $K_0 = 5$; curve 7, $K_0 = 10$; curve 8, $K_0 = 50$; curve 9, $K_0 = 100$; curve 10, $K_0 = \infty$.

2.1.2. Dynamic quenching

Let φ_1 denote the configurational distribution function

$$\varphi_{1(\rho,0)} = \langle \varphi \rangle = L \frac{\exp(-K_0^{1/2}\rho)}{\rho}$$

where L is a normalizing distance.

The evolution of φ_1 is given by

$$(\varphi_1)_R = 0$$

and for $\rho \geqslant R$

$$\frac{\partial \varphi_1}{\partial \tau} = \frac{\partial^2 \varphi_1}{\partial \rho^2} + \frac{2}{\rho} \frac{\partial \varphi_1}{\partial \rho}$$

which leads, in Laplace space, to

$$\left(\frac{dy_1}{d\rho}\right)_R = \frac{L}{s^{1/2} + K_0^{1/2}} \frac{\exp(-K_0^{1/2}R)}{R}$$

As

$$\frac{dB(T_1)}{dt} = -4\pi N\sigma RD\left(\frac{\partial \varphi_1}{\partial \rho}\right)_1$$

we obtain the following yield of dynamic quenching:

$$DQ = \frac{RK_0^{1/2}}{1 + K_0^{1/2}} \exp\{-K_0^{1/2}(R-1)\} \frac{1}{1 - SQ}$$

2.1.3. Overall quenching

The overall quenching is given by the sum of the static and the dynamic quenching:

$$GQ = \frac{K_0^{1/2}(R-1) + 1}{K_0^{1/2} + 1} \exp\{-K_0^{1/2}(R-1)\}$$

2.2. Model including concepts from liquid physics

Experiments can be interpreted using the preceding model. However, as it has already been pointed out in ref. 4, data obtained for a hydrocarbon solvent of low viscosity do not agree with the model.

Thus the model developed in ref. 4 can only be considered as a model that can reproduce trends. In order to refine the model, we have initially taken into account some concepts from the liquid physics of diffusion-controlled reactions. These models, for simple liquids, show that the radial distribution functions $g(r)$ are obviously not uniform, particularly in the vicinity of the collision distance between the two reactants. This leads to an important modification of the kinetic results that are summarized below.

2.2.1. Radial distribution function and diffusion model of a reaction with a homogeneous distribution

Consider the case of a homogeneous system of spherical molecules B, in an inert solvent S composed of spherical molecules of the same size. At $t = 0$, excitation with light, for example, generates very reactive A molecules which have the same properties as B and S but are reactive towards B. If we consider that *every* A–B encounter leads to a chemical reaction whose lifetime is taken to be nearly zero, it is possible to calculate the apparent rate constant $k_a(t)$ of the reaction by solving the classical equation

$$\frac{\partial \varphi}{\partial t} + \mathcal{G}\varphi = 0$$

where $\mathcal{G}$ is a time evolution operator.

Let ψ be the apparent potential between A, B and S; $\mathcal{G}$ is then given by [6]

$$\mathcal{G}X = -(D\,\nabla^2 X + K\,\nabla X \cdot \nabla\psi + KX\,\nabla^2\psi)$$

where the mobility coefficient $K = D/kT$ is given by the Nernst–Einstein equation.

2.2.1.1. Dilute solution. As the molecular density $\bar{\rho}$ approaches zero, we must solve the equation

$$\frac{\partial \varphi}{\partial t} = D\,\nabla^2\varphi$$

to give an analytical expression

$$k_a(t) = 4\pi N\sigma^2 D\left(\frac{\partial \varphi}{\partial r}\right)_\sigma = 4\pi N\sigma D\left\{1 + \frac{\sigma}{(\pi Dt)^{1/2}}\right\}$$

for the apparent rate constant. At $\sigma = 0$, $\varphi(r/\sigma, 0) = 1$ for $r/\sigma = \rho > 1$ and we have to solve

$$sy - 1 = y'' + \frac{2}{\rho}y'$$

with

$$y = \int_0^\infty \exp(-s\tau)\varphi(\rho,\tau)\,d\tau$$

and

$$\tau = \frac{Dt}{\sigma^2}$$

This leads to

$$y = \frac{1}{s}\left[1 - \frac{\exp\{-s^{1/2}(\rho - 1)\}}{\rho}\right]$$

$$y'(1) = \frac{1}{s} + \frac{1}{s^{1/2}}$$

and

$$\left(\frac{d\varphi}{d\rho}\right)_1 = 1 + \frac{1}{(\pi\tau)^{1/2}} = 1 + \frac{\sigma}{(\pi Dt)^{1/2}}$$

2.2.1.2. Realistic solution. Many authors have already studied systems of hard-core molecules [9 - 13]. Generally, we can define a total correlation function $h(r) = g(r) - 1$ where $g(r)$ is the radial distribution function and, from Ornstein and Zernike [14], a direct correlation function $c(r)$ by

$$h(r_{12}) = c(r_{12}) + \bar{\rho}\int_{r_3} h(r_{13})c(r_{23})\,dr_3$$

with

$$r_{ij} = |r_i - r_j|$$

The above integral is the convolution of $h(r)$ and $c(r)$. It gives the correlation of molecules 1 and 2, through the action of a third molecule. The hard-sphere approximation consists in setting $c(r) = 0$ and $r > \sigma$, following Percus and Yevick [9].

It can be shown [15] that the Laplace transform of $g(r)$ is

$$G(s) = \frac{sL(s)}{12\bar{\eta}\{L(s) + \exp(s)S(s)\}}$$

with

$$\bar{\eta} = \frac{\pi\bar{\rho}\sigma^3}{6}$$

$$L(s) = 12\bar{\eta}\left\{1 + 2\bar{\eta} + s\left(1 + \frac{\bar{\eta}}{2}\right)\right\}$$

and

$$S(s) = -12\bar{\eta}(1 + 2\bar{\eta}) + 18\bar{\eta}^2 s + 6\bar{\eta}(1 - \bar{\eta})s^2 + (1 - \bar{\eta})^2 s^3$$

Smith and Henderson [16] have inverted this relation to obtain $g(r)$ directly. But, for simplicity, we first transform $G(s)$ into $G(\omega)$ ($s = i\omega$) and then return to real space by using the fast Fourier transform (FFT) algorithm [17]. This algorithm requires that the function being inverted approaches zero when $s = 0$ and $s \to \infty$. The $G(s)$ do not obey this condition and we must consider the function

$$H(s) = G(s) - \exp(-s)\left(\frac{1}{s} + \frac{1}{s^2}\right)$$

where $\exp(-s)(1/s + 1/s^2)$ is the Laplace transform of $rU(r - 1)$, where $U(x)$ is defined by

$U(x) = 1$ for $x > 0$

$U(x) = 0$ for $x < 0$

$H(s)$ is then a "good" function and we can apply the FFT algorithm. Then we just have to subtract $rU(r - 1)$ to obtain $g(r)$ numerically. Figure 3 shows some examples of such curves for two values of η.

Since the system is thermodynamically stable, we must have

$$\frac{dg}{dt} + \mathcal{G}g = 0 \quad \text{for } t \geqslant 0$$

which leads to $g(r) = \exp\{-\psi(r)/kT\}$ and allows us to calculate the apparent potential ψ/kT.

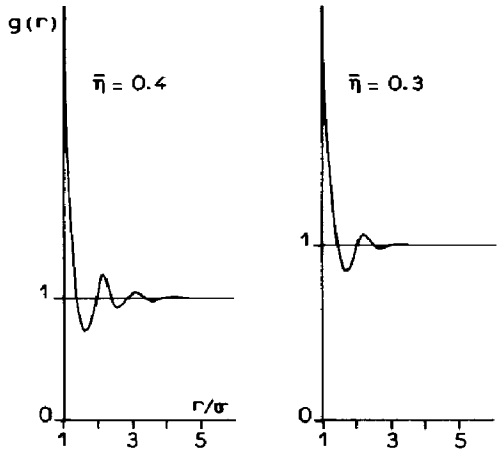

Fig. 3. Radial distribution function for two values of η.

2.2.1.3. Dimensionless relations and simplified model. At time $t = 0$, when A molecules are created, the distribution of B around A is represented by $g(r)$ (after multiplication by a coefficient $\langle B \rangle$). Subsequently, every time a B molecule encounters an A molecule there will be a reaction followed by the disappearance of the interacting species. Under these conditions, the apparent rate constant of the reaction between A and B is

$$\bar{k}_a(t) = 4\pi N\sigma^2 D\left(\nabla\varphi_\sigma + \varphi_\sigma \frac{\nabla\psi}{kT}\right)$$

with

$$\varphi_\sigma = 0$$

leading to

$$\bar{k}_a(t) = 4\pi N\sigma^2 D\left(\frac{\partial\varphi}{\partial r}\right)_\sigma$$

Putting $y = \varphi(r,t)/\varphi(r,0)$, $\rho = r/\sigma$ and $\tau = Dt/\sigma^2$, if D is assumed to remain constant on varying r, we must solve the following simplified system:

$$\frac{dy}{d\tau} = \frac{d^2y}{d\rho^2} + \frac{dy}{d\rho}\left(\frac{2}{\rho} - \frac{d\bar{\psi}}{d\rho}\right)$$

with

$$\bar{\psi} = \frac{\psi}{kT}$$

and

$y(\rho) = 1$ for $\rho > 1$ and $t = 0$

$y(1) = 0$ for $t > 0$

$\bar{\psi}$ is not a stationary function and we cannot solve this simplified equation through using any transform (Fourier or Laplace). For these reasons, we have solved the above system by numerical integration, using a network method: the space is cut up into intervals Δr_i over which $\bar{\psi}(r)$ is assumed to be constant. We then have a linear system which can be solved in Laplace space, taking into account the continuity of y and $dy/d\rho$ at the links in the network. Returning to real space is achieved as already discussed.

2.2.1.4. Time evolution of the flux. The apparent rate constant of reaction is given by

$$\bar{k}_a(\tau) = 4\pi N\sigma D\left(\frac{\partial y}{\partial \rho}\right)_1 \exp\{-\bar{\psi}(1)\}$$

Figure 4 shows the variation of $\mathcal{R}(\tau) = \bar{k}_a(\tau)/k_a(\tau)$ with τ for two values of $\bar{\eta}$.

Generally, $\mathcal{R}(\tau)$ is nearly always a decreasing function which converges to an asymptotic value $\mathcal{R}_\infty$ that is greater than unity and dependent on $\bar{\eta}$.

Moreover, near $t = 0$, $\mathcal{R}_0$ is approximately given by

$$\mathcal{R}_0 = \exp\{-\bar{\psi}(1)\} = g(1)$$

This implies an initial flux much larger than that obtained by employing a uniform radial distribution function.

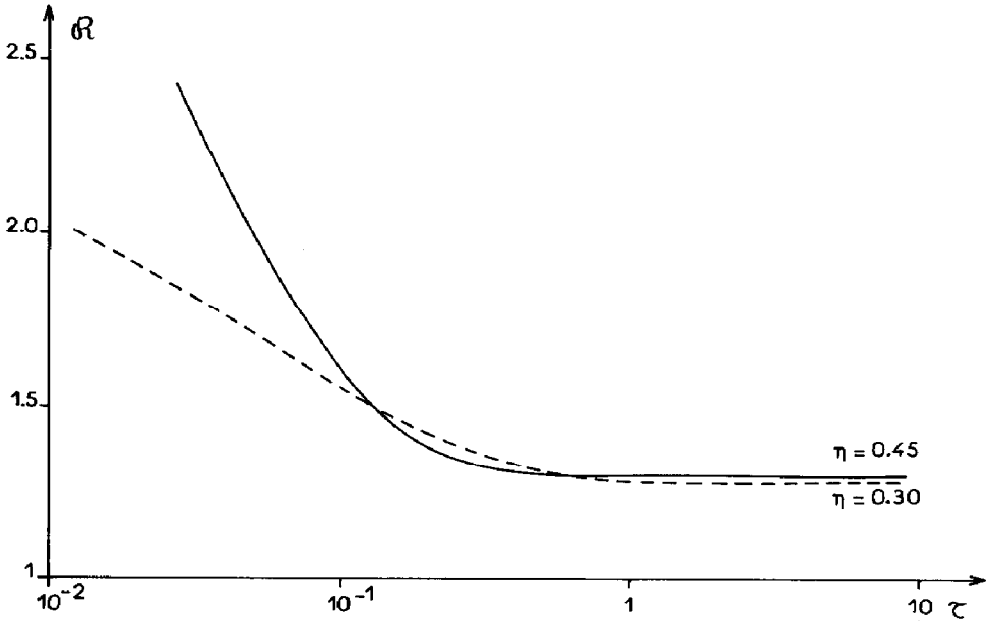

Fig. 4. Variation in $\mathcal{R}(\tau)$ *vs.* τ for two values of η.

2.2.2. Case of a non-uniform distribution

Concepts from liquid physics can be used in the case where the initial configuration of B around A is identical with that existing at the time of the first energy transfer ($A^*(S_1) + B \rightarrow B^*(S_1) + A$, for example). From the apparent potential defined for hard spheres, we must solve the system

$$\frac{\partial \varphi}{\partial t} + \mathcal{G}\varphi = 0$$

with the conditions

$$\left(\frac{\partial \varphi}{\partial \rho}\right)_1 = 0$$

and

$$\int_{\sigma}^{\infty} \varphi \, d\upsilon = 1$$

This system can easily be solved by a numerical network method, leading to a representation of $\varphi(\rho,\tau)$ (see Fig. 5). We must calculate a mean value at the time when $B^*(T_1)$ is created, which is given by

$$\langle \varphi \rangle = \int_0^{\infty} k_0 \exp(-k_0 t)\varphi(\rho,t) \, d\tau$$

Now, contrary to when φ can be expressed in a transform space such as Laplace space, $\langle \varphi \rangle$ must be calculated by numerical integration for each value of $k_0\sigma^2/D$. For this reason and in view of the difficulties of obtaining more accurate experimental data, we have tried to transform the physical system so that an expression for $\langle \varphi \rangle$ can be obtained.

2.2.3. Simplified system

Let us consider, for the case of a diffusion-controlled reaction, the existence of an apparent potential with discrete values, as plotted in Fig. 6, which is consistent with the concepts from liquid physics as defined above: it is assumed that

$\varphi = P$ for $\rho \in [1,R]$

$\varphi = 1$ for $\rho > R$

Using this potential, we can solve $\partial\varphi/\partial t + \mathcal{G}\varphi = 0$ and find a simplified solution in Laplace space. If y is the Laplace transform of $\varphi \exp(-\psi)$, two functions can be calculated:

y_1 for $\rho \in [1,R]$

y_2 for $\rho > R$

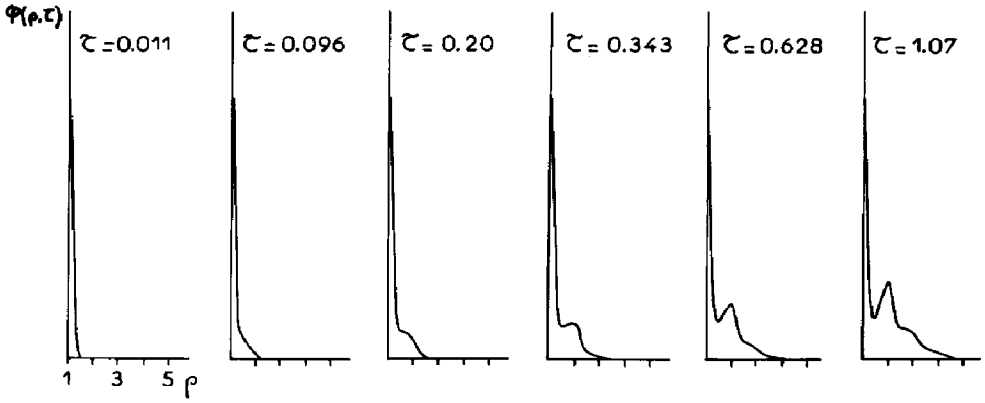

Fig. 5. Variation in $\varphi(\rho,\tau)$ *vs.* ρ and τ for $\eta = 0.5$.

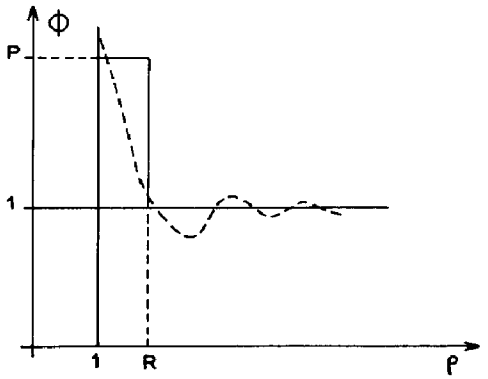

Fig. 6. Simplified model (see text).

with the limiting conditions

$(y_1)_R = (y_2)_R$

$$P\left(\frac{dy_1}{d\rho}\right)_R = \left(\frac{dy_2}{d\rho}\right)_R$$

For a totally diffusion-controlled reaction, we have

$(y_1)_1 = 0$

From these considerations, the expression f for the flux of B towards A in Laplace space is

$$f(s) = \frac{P}{s}\left[\frac{(s^{1/2}+1)\{(P+1)s^{1/2}R-(P-1)\}\exp\{2s^{1/2}(R-1)\}}{(P-1)(s^{1/2}R+1)} - (s^{1/2}-1)\right] \times$$

$$\times\left[1+\frac{(P+1)s^{1/2}R-(P-1)}{(P-1)(s^{1/2}R+1)}\exp\{2s^{1/2}(R-1)\}\right]^{-1}$$

It is not easy to calculate the corresponding function in time space by classical methods although it is possible by using an FFT. However, in view of the simplifying assumptions already made, here we have only examined the flux at large times; this allows us to take a Taylor expansion of $f(s)$, giving the simple expression

$$f(s) \approx \frac{RP}{s(R+P-1)}\left(1 + \frac{RP}{R+P-1}\, s^{1/2}\right) + \ldots$$

which can be easily inverted, giving

$$k(t) = 4\pi N\sigma D \frac{RP}{R+P-1}\left\{1 + \frac{RP}{R+P-1}\,\frac{\sigma}{(\pi Dt)^{1/2}}\right\} + \ldots$$

This means that $k(t)$ only depends on the parameter $RP/(R+P-1)$. Comparing this expression with the numerical expression obtained by numerical integration, for the case of hard spheres, we can reasonably adjust the two kinds of functions, as is shown in Fig. 7. This enables us to replace the physical system by a simple system, which is easier to handle mathematically and leads to kinetic results which are very similar.

Starting with the above simplifying assumptions, we propose a model for the transport out of the cage. Let us consider two regions

for $\rho \in [1,R]$, function φ_1

for $\rho > R$, function φ_2

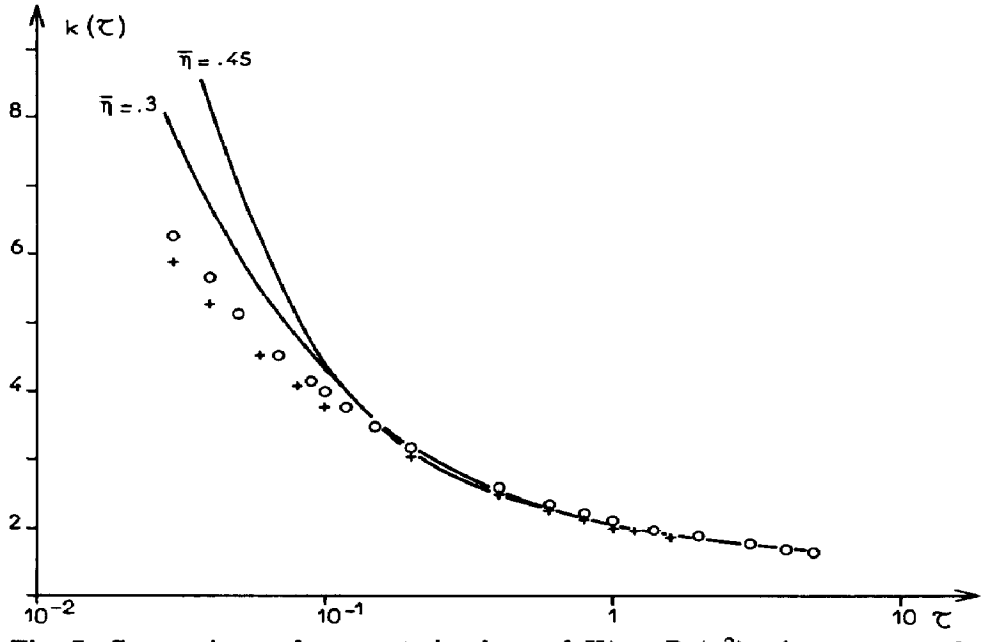

Fig. 7. Comparison of computed values of $K(\tau = Dt/\sigma^2)$ using concepts from liquid physics (full line) with the expression of Section 2.2.3: ○, $RP/(R+P-1) = 1.24$; +, $RP/(R+P-1) = 1.2$.

and assume that the species are in contact at time $t = 0$. In the Laplace space we thus obtain

$$y_1 = A_1 \frac{\exp(-s^{1/2}\rho)}{\rho} + B_1 \frac{\exp(s^{1/2}\rho)}{\rho} \quad \text{for } \rho \in [1,R]$$

$$y_2 = A_2 \frac{\exp(-s^{1/2}\rho)}{\rho} \quad \text{for } \rho > R$$

with

$$A_1 = C_1 B_1$$

$$A_2 = \frac{1}{P}\{C_1 + \exp(2s^{1/2}R)\}B_1$$

$$C_1 = \frac{1}{P-1}\left\{1 + \frac{Ps^{1/2}R - 1}{s^{1/2}R + 1} \exp(2s^{1/2}R)\right\}$$

$$\frac{1}{B_1} = NV_0 \{\exp(-s^{1/2}R)(Rs^{1/2} + 1)\}\left\{C_1 \frac{(1-P)}{P} + \frac{\exp(2s^{1/2}R)}{P}\right\} +$$

$$+ \exp(s^{1/2}R)(Rs^{1/2} - 1) + C_1 \exp(-s^{1/2})(s^{1/2} + 1) - \exp(-s^{1/2})(s^{1/2} - 1)$$

As above, we choose a mean value of φ weighted by $K_0 \exp(-K_0\tau)$:

$$\langle \varphi_1 \rangle_t = 0 = K_0 y_1(K_0)$$

$$\langle \varphi_2 \rangle_t = 0 = K_0 y_2(K_0)$$

Starting with this initial configuration it is then possible to calculate the time evolution of the flux by solving

$$\frac{\partial \varphi}{\partial \tau} + \mathcal{G}\varphi = 0$$

with the condition $\varphi_{\rho=1} = 0$.

For this study, it does not seem important to take into account the static quenching term. However, this can be done by making the same assumption as in Section 2.

In Laplace space, the derivation of φ is given by

$$\mathcal{L}\left(\frac{d\varphi}{d\rho}\right)_1 = F = -\alpha_1(s^{1/2} + 1)\exp(-s^{1/2}) + \beta_1(s^{1/2} - 1)\exp(s^{1/2}) + \frac{K_0}{K_0 - s} A_1 \times$$

$$\times (K_0^{1/2} + 1)\exp(-K_0^{1/2}) - \frac{K_0}{K_0 - s} B_1 (K_0^{1/2} - 1)\exp(K_0^{1/2})$$

where α_1, β_1, A_1 and B_1 are functions of s independent of ρ, and F is a dimensionless flux (see Appendix A).

The reaction yield in the enlarged cage is calculated in the way previously described. We calculate the amount Y which reacts using

$$Y = \int_0^\infty 4\pi\sigma^2 D \left(\frac{\partial\varphi}{\partial\rho}\right)_1 dt$$

which, with a multiplication factor $4\pi\sigma^2 D$, is the limit of sF when s approaches zero. This calculation has been computed and leads, for example, to the results collected in Fig. 8. These show that the values of P and R have an important effect on the yield of energy transfer.

The two models are compared in Section 3.

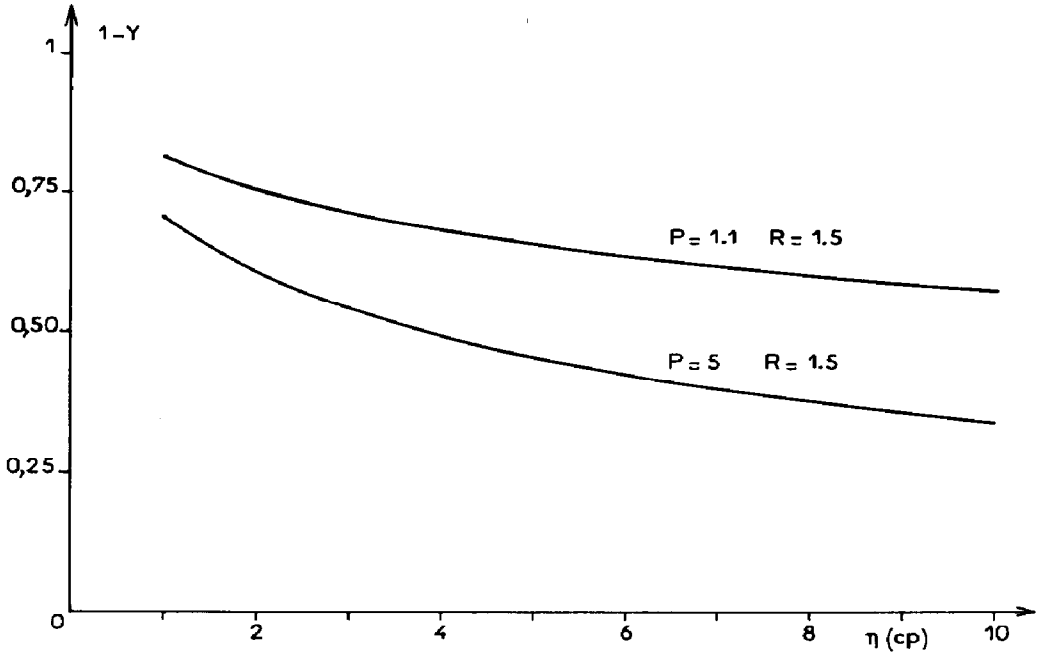

Fig. 8. Variation in $1 - Y$ (Y, yield of double transfer) *vs.* the viscosity η for two sets of parameters R and P.

3. Experimental results and discussion

In a recent paper, we presented a simplified model for a diffusion-controlled reaction with a double energy transfer and gave pyrene–biacetyl as an experimental example [4]. We found quite a good agreement between the experimental trends and those of the model, concerning the transfer yield in the enlarged cage. A pyrene molecule transfers its energy to singlet biacetyl. This energy raises the biacetyl to its triplet state and it can then transfer the energy to the original pyrene molecule, if it has not diffused out

of the cage [3]. In Section 2, we proposed a simple model by employing elementary concepts from liquid physics. We considered that molecules are hard spheres and that there is no potential between them.

In order to check the generality of the process of double transfer and to improve the modelling of such reactions, we have studied reactions occurring in an enlarged cage: between pyrene, 9,10-diphenylanthracene, 1,2,5,6-dibenzanthracene or 1,2-benzanthracene (A) and biacetyl (B). These substances A and B indeed have energy levels such that the transfers $A(S_1) + B \rightarrow B(S_1) + A$ and $B(T_1) + A \rightarrow A(T_1) + B$ are exoenergetic and very efficient (Fig. 1). Moreover, biacetyl is a particularly interesting molecule which emits both fluorescence and phosphorescence in solution. Lastly, measurements were made in different media of different viscosity. The experimental results indicate the obvious general trend already established in ref. 4. It is possible to show that the model employing concepts from liquid physics leads to results which agree better with physical reality than do those using the simplified model (see ref. 4 and Section 2).

3.1. Experimental details

3.1.1. Products and materials

Solvents (cyclohexane (Spectrosol), paraffin oil (Uvasol) and cyclohexanol (Fluka)) and aromatic compounds (purissimum from Fluka) were used without purification. Biacetyl (purissimum from Fluka) was vacuum distilled in order to remove polymers. Solutions were carefully degassed by performing four freeze–pump–thaw cycles to ensure the absence of oxygen in the measuring cell. Spectrofluorometry and spectrophosphorometry experiments were carried out using a JY3 spectrofluorometer from Jobin–Yvon, ISA division. Typically, spectral widths of 10 nm were used for both excitation and analysis. Measurements were made at room temperature (20 °C) and the viscosity was determined, at the same temperature, with a Prolabo automatic viscosimeter.

3.1.2. Technique for the measurement of the transfer yield for $B^*(T_1) \rightarrow A^*(T_1)$

Two experiments were carried out: (i) excitation at $\lambda = 420$ nm of biacetyl in order to study the transfer $B^*(T_1) \rightarrow A^*(T_1)$ without double transfer; (ii) excitation at $\lambda = 335$ nm of the aromatic compound A in order to study the effect of double transfer. Variations in fluorescence and phosphorescence intensities were then compared, as discussed below, allowing the calculation of the yield Y of double transfer.

The fluorescence of biacetyl was monitored at 470 nm and its phosphorescence was monitored at 520 nm (Fig. 9). By exciting biacetyl at 420 nm, we measured the intensities I_{470}^{420} and I_{520}^{420} leading to a ratio of emissions: $P_0 = I_{520}^{420}/I_{470}^{420}$.

When excited at 335 nm biacetyl absorbs part of the exciting light. The phosphorescence at 520 nm includes a component I_{520}^{d} due to direct

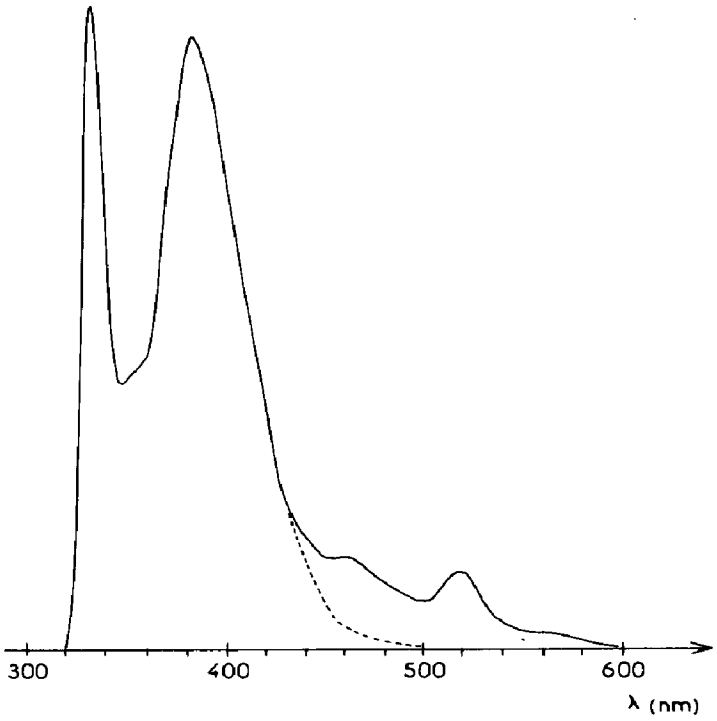

Fig. 9. Emission spectra of a mixture of biacetyl (2×10^{-2} M) and pyrene (10^{-6} M) in 30vol.%cyclohexane–70vol.%paraffin oil (λ_{exc} = 335 nm). The broken line indicates the contribution of pyrene alone.

excitation, which can be deduced from the fluorescence intensity I_{470}^{335} at 470 nm after subtraction of the aromatic contribution according to

$$I_{520}^{d} = P_0 I_{470}^{335} \frac{\beta[B]}{\alpha[A] + \beta[B]}$$

where α and β are the absorption coefficients of A and B respectively.

The total phosphorescence intensity I_{520}^{335} is the sum of I_{520}^{d} and of the sensitized component I_{520}^{s}. Then

$$I_{520}^{s} = I_{520}^{335} - \frac{I_{520}^{420}}{I_{470}^{420}} I_{470}^{335} \frac{\beta[B]}{\alpha[A] + \beta[B]}$$

The yield Y of double transfer is expressed by

$$Y = 1 - \frac{I_{520}^{s}}{I_{470}^{s}} \frac{I_{470}^{420}}{I_{520}^{420}}$$

and can be calculated from the above relationships. However, it must be pointed out that certain constraints appear in carrying out such an experiment; indeed, it is necessary, for simplicity, to work under conditions such that the emission is nearly linearly proportional to the concentration of the reagents A and B. This implies an optical density, at the excitation wavelength, lower than about 0.2. This condition leads to limitations of the

concentration, mainly for biacetyl, which absorbs only weakly at 335 nm. The viscosity cannot then be varied over too large a range. Indeed, the reaction $A^*(S_1) + B$ must also be allowed, which is difficult to measure in media which are too viscous.

3.1.3. Study of the reaction $A^*(S_1) + B$

The reaction $A^*(S_1) + B$ is well known and allows the estimation of the quantity of energy transferred to biacetyl by measurement of the fluorescence quenching of A^* *versus* [B].

3.1.4. Lifetimes of singlet excited states

The lifetimes of the singlet excited states were measured by time-resolved spectroscopy with correlated single-photon counting, using partly home-made apparatus. Lifetimes were calculated by iterative reconvolution.

3.2. Experimental results

Measurements were carried out for different aromatic compound–biacetyl pairs in mixtures of hydrocarbons or in cyclohexane–cyclohexanol mixtures.

3.2.1. Study of the reaction $A^*(S_1) + B$

The study of the reaction $A^*(S_1) + B$ is actually complementary to the subject matter of this paper, but the experiments that have been performed allow us to begin a kinetic analysis of this first energy transfer when excitation is continuous. Figure 10 shows the variations in the product $K_{sv}\eta$ *versus* η (where K_{sv} is the Stern–Volmer constant and η is the viscosity of medium) in cyclohexane–paraffin mixtures. It is clear that $K_{sv}\eta$ is constant with η for the pyrene–biacetyl pair. It has already been shown that the kinetics of the reaction pyrene(S_1) plus biacetyl is diffusion controlled [9]. This result

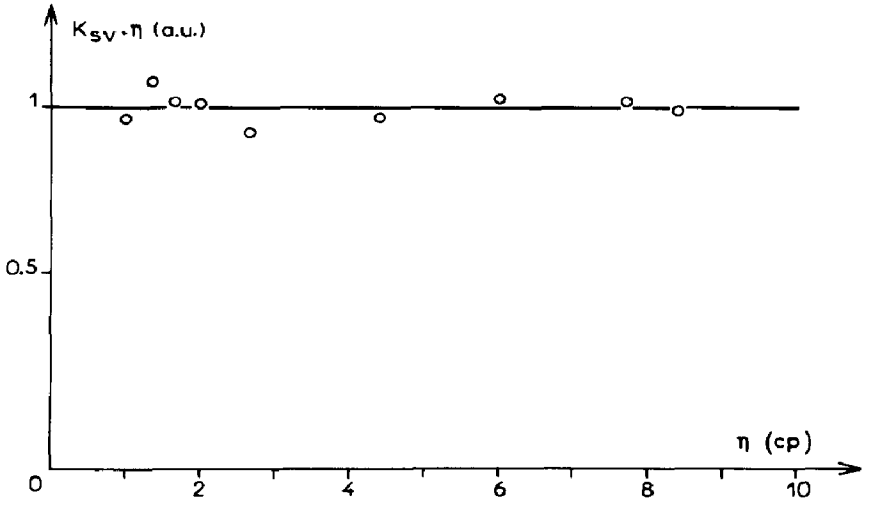

Fig. 10. Variation in $K_{sv}\eta$ *vs.* η in mixtures of cyclohexane and paraffin.

enables us to assume that Stokes' law is approximately obeyed. However, this assumption must be made with care as, under continuous excitation, two effects, resulting from static and dynamic quenching, can appear. For this reason, measurements with pulsed excitation have been undertaken. They should enable a better understanding of the relationship between the diffusivity D and the viscosity η in the solvents of interest.

3.2.2. Double energy transfer

Figure 11 shows the variations in the fluorescence and phosphorescence spectra of biacetyl either sensitized by electronically excited pyrene or directly excited at 420 nm (at which pyrene is transparent). Figure 11 clearly indicates that the phosphorescence of biacetyl relative to its fluorescence is smaller when biacetyl is sensitized by pyrene than when it is directly excited. This result is due to double energy transfer.

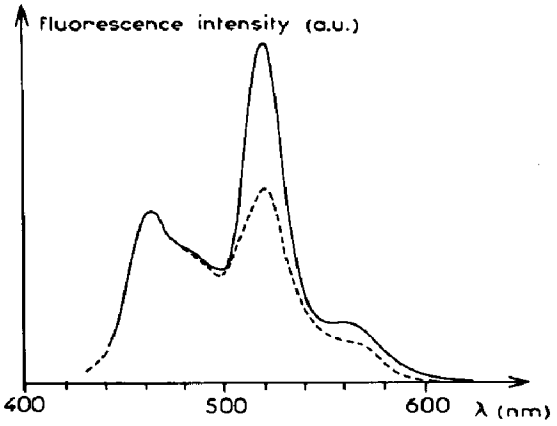

Fig. 11. Emission spectra of biacetyl (solvent, degassed cyclohexane–paraffin mixture ($\eta \approx 9$ cP); [biacetyl] = 10^{-2} M; [pyrene] = 10^{-6} M): full line, direct excitation of biacetyl (λ_{exc} = 420 nm); broken line, sensitization by pyrene (λ_{exc} = 335 nm).

Figure 12 illustrates variations in the yield Y of double transfer (defined in Section 3.1.2) *versus* η for all the aromatic compounds used in the presence of biacetyl and for cyclohexane–paraffin mixtures. We note that, within the experimental accuracy, these products react in the same way with biacetyl.

The choice of solvent does not seem to be of major importance as the effect of η on Y when the solvent is a mixture of cyclohexane and cyclohexanol is practically identical with that when the solvent is a cyclohexane–paraffin mixture, as shown in Fig. 13.

3.3. Interpretation of the experimental results

In ref. 4 we proposed a simple kinetic model in which we assumed a chemical reaction distance $R\sigma$ (σ being the collision distance). Starting from the fact that A molecules present between σ and $R\sigma$ interact immediately with $B(T_1)$, it is possible to obtain a simplified expression

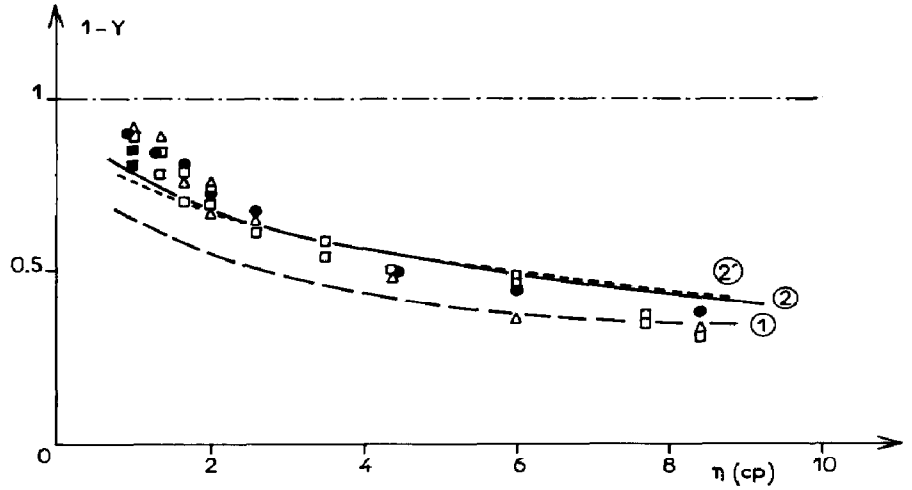

Fig. 12. Variations in $1 - Y$ (Y, yield of double transfer) *vs.* η in cyclohexane–paraffin mixtures: curve 1, simplified model; curve 2, with the assumption of a non-uniform radial distribution function ($P = 7.5$, $R = 1.25$ and $\sigma = 6$ Å); curve 2', as curve 2 with $P = 6.2$, $R = 1.2$ and $\sigma = 7$ Å. Aromatic compounds: □, pyrene; ●, 1,2-3,4-dibenzoanthracene; △, 1,2-benzanthracene; ■, diphenylanthracene.

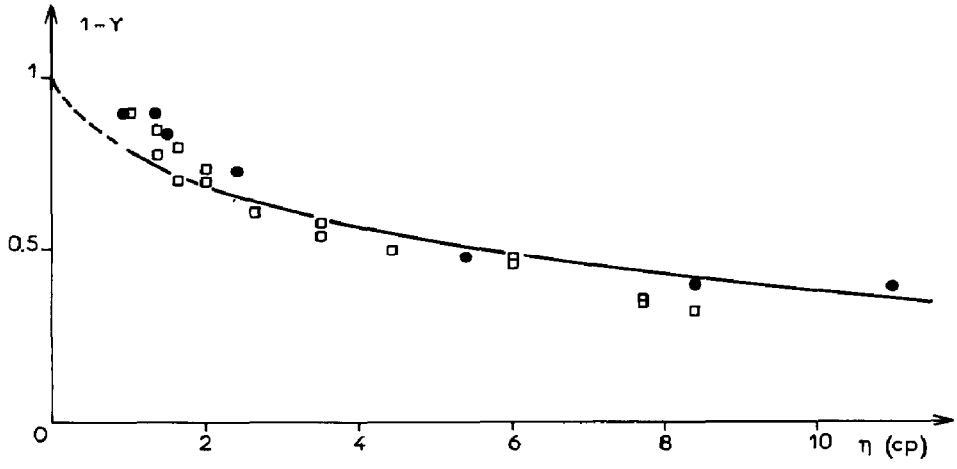

Fig. 13. Variations in $1 - Y$ (Y, yield of double transfer) *vs.* η in cyclohexane–cyclohexanol mixtures (●) and in cyclohexane–paraffin mixtures (□) (aromatic compound, pyrene).

$$Y = GQ = \frac{K_0^{1/2}(R-1)+1}{K_0^{1/2}+1} \exp\{-K_0^{1/2}(R-1)\}$$

for the yield of double transfer, in which $K_0 = k_0\sigma^2/D$, k_0 is the monomolecular rate constant of intersystem transition for biacetyl and D is the mutual diffusion coefficient of A and B.

This very simple model assumes uniform radial distribution functions, which is the case for media of low density with no potential between reactants and solvent. Moreover, the molecules are assumed to be spherical. The graphs shown in Fig. 11 indicate that it is possible to find a satisfactory fit between this simplified model and the experimental results. Assuming

$k_0 = 10^8\ s^{-1}$ and the validity of the Stokes law, we calculate an R value of about 1.6, which gives a chemical reaction distance of about 10 Å. It is usual to find values of the reaction distance $R\sigma$ much larger than the collision distance σ in investigations of fluorescence quenching following diffusion-controlled kinetics. However, knowing the overlap integrals between reactants, it can be shown that for such distances this overlap is nearly zero, which makes energy transfer unlikely. Discrepancies between the experimental results and the model can arise from phenomena which have not been taken into account in the model, such as interaction potentials and radial distribution functions. The calculation of the interaction potential is quite tedious, but in Section 2.2.3 we have been able to develop a model including, in a simple way, some of the concepts from liquid physics, leading to an expression for Y in terms of the two parameters R and P ($P > 1$ between 1 and R). Calculations have been carried out without the assumption of static quenching. Now, as it is shown in Figs. 12 and 13, numerical adjustment of these two parameters leads to good agreement between the experimental results and the model. However, for small values of the viscosity η, a discrepancy still remains but is of less importance. Under our conditions, the most probable values of R and P (which have a physical significance contrary to a very large chemical reaction distance) are

$$\left.\begin{matrix} P = 7.5 \\ R = 1.25 \end{matrix}\right\} \sigma = 6\ \text{Å} \qquad \left.\begin{matrix} P = 6.2 \\ R = 1.2 \end{matrix}\right\} \sigma = 7\ \text{Å}$$

Discrepancies at small values of η can have different explanations: (i) local potentials between excited molecules and reagents or solvents; (ii) variations in the mutual diffusion coefficient with distance; (iii) a non-totally diffusion-controlled reaction between $B^*(T_1)$ and A; (iv) partial non-validity of the Stokes law etc.

It is possible to take these different physical conditions into account in a new model, but this requires fixing these conditions *a priori* in order to reduce the number of dynamic parameters to a minimum. These considerations suggest some further experiments, and these are in progress at present. However, we believe that the model developed in this paper enables us to explain the main features of the double transfer phenomenon, with no assumption for the chemical reaction distance.

References

1 T. Koenig, *J. Am. Chem. Soc.*, *91* (1969) 2558.
2 J. C. André, A. Tournier, M. Bouchy and X. Deglise, *React. Kinet. Catal. Lett.*, *17* (1981) 433.
3 J. C. André, M. Bouchy and W. R. Ware, *Chem. Phys.*, *37* (1979) 119.
4 J. Rima, M. Bouchy, J. C. André and M. L. Viriot, *Chem. Phys. Lett.*, *106* (1984) 333.
5 D. L. Dexter, *J. Chem. Phys.*, *21* (1953) 836.

6 J. C. André, M. Niclause and W. R. Ware, *Chem. Phys.*, *28* (1978) 371.
7 B. Stevens, *J. Phys. Chem.*, *85* (1981) 3552.
8 J. C. André and M. Bouchy, to be published.
9 J. K. Percus and G. J. Yevick, *Phys. Rev.*, *110* (1958) 1.
10 J. L. Lebowitz, *Phys. Rev. A*, *133* (1964) 895.
11 R. J. Baxter, *Aust. J. Phys.*, *21* (1968) 563.
12 L. Verlet and J. J. Weis, *Phys. Rev. A*, *5* (1972) 939.
13 Y. T. Lee, F. H. Ree and T. Ree, *J. Chem. Phys.*, *55* (1971) 234.
14 L. S. Ornstein and F. Zernike, *Proc. Acad. Sci. Amsterdam*, *17* (1914) 793.
15 H. Eyring, D. Henderson, B. J. Stover and E. M. Eyring, *Statistical Mechanics and Dynamics*, Wiley-Interscience, 1982.
16 W. R. Smith and D. Henderson, *Mol. Phys.*, *19* (1970) 411.
17 J. Bordet, in M. Bouchy (ed.), *Deconvolution and Reconvolution of Analytical Signals*, Nancy, 1982, pp. 123 - 143.

Appendix A

F is calculated as follows. If $u = s^{1/2}$ we define

$$\gamma(u) = A_1 \exp(-K_0^{1/2}R)\left(K_0^{1/2}R + 1 - \frac{uR+1}{P}\right) - B_1 \exp(K_0^{1/2}R) \times$$

$$\times \left(K_0^{1/2}R - 1 + \frac{uR+1}{P}\right) + \frac{A_2 \exp(-K_0^{1/2}R)(uR - K_0^{1/2}R)K_0}{K_0 - u^2}$$

$$\alpha_0(u) = \frac{\{uR(P+1) - (P-1)\} \exp(2uR)}{(P-1)/(uR+1)}$$

$$\beta_1(u) = \left[\frac{-\gamma(u)P \exp(uR)}{(P-1)(uR+1)} + \frac{K_0\{A_1 \exp(-K_0^{1/2} + u) + B_1 \exp(K_0^{1/2} + u)\}}{K_0 - u^2}\right] \times$$

$$\times \{\alpha_0(u) + \exp(2u)\}^{-1}$$

$$\alpha_1(u) = \alpha_0(u)\beta_1(u) + \frac{\gamma(u)P \exp(uR)}{(P-1)(uR+1)}$$

$$F(u) = -\alpha_1(u)(u+1) \exp(-u) + (u-1)\beta_1 \exp(u) +$$

$$+ \frac{K_0 A_1(K_0^{1/2} + 1) \exp(-K_0^{1/2})}{K_0 - u^2} - \frac{K_0 B_1(K_0^{1/2} - 1) \exp(K_0^{1/2})}{K_0 - u^2}$$